

Plasma Diagnostics and Elemental Abundance Determinations for PNe – Current Status

Xiao-wei Liu

Department of Astronomy, Peking University, Beijing 100871, P. R. China

1 Overview

Much of our knowledge of elemental abundances in our own and other galaxies rests on photoionized gaseous nebulae, such as H II regions and planetary nebulae (PNe). The current paper deals with the two related long-standing problems in nebular astrophysics, whereby electron temperatures derived from the hydrogen recombination spectrum Balmer discontinuity are systematically lower than values deduced from the collisionally excited [O III] nebular to auroral line ratio, and whereby heavy element abundances relative to hydrogen deduced from optical recombination lines (ORLs) are systematically higher than those determined from collision excited lines (CELs). We concentrate on results from bright Galactic PNe. Observations of extragalactic PNe are scarce due to the difficulty of detecting faint ORLs from heavy element ions. The situation is however changing rapidly with the wide deployment of 10m class telescopes and sophisticated spectrographs.

Deep optical spectrophotometry, allowing plasma diagnostics and abundance determinations using weak nebular continuum emission and ORLs emitted by heavy element ions, has now been carried out for several dozen Galactic PNe and a few Magellanic Cloud PNe. The results show that the ORL to CEL temperature and abundance determination disparities are ubiquitous. Many PNe have also been observed in the IR using the Infrared Space Observatory (ISO), giving access to fine-structure lines (FSLs), crucial to discriminate various scenarios for the causes of the disparities, including temperature fluctuations, density inhomogeneities and abundance variations. It is shown that temperature fluctuations and density inhomogeneities fail to provide a self-consistent explanation of observations and that there is strong evidence pointing towards the presence of a new ultra-cold plasma, highly enriched in helium and heavy elements and probably in the form of H-deficient knots, embedded in the nebula. Section 2 reviews some basic properties of CELs and ORLs. Observations of ORLs are summarized in Section 3 and elemental abundances derived from ORLs are compared to those derived from CELs in Section 4. Temperature, density and abundance inhomogeneities as the possible causes of the ORL to CEL discrepancies are discussed in Section 5. The nature and origins of H-deficient knots are discussed in the last Section.

Recent reviews on this topic are given by Liu (2002, 2003), Esteban (2002), Peimbert (2002), Torres-Peimbert & Peimbert (2003). A general review on the physics of emission line nebulae is given by Ferland (2003).

2 Recombination and Collisional excitation

Ionized and heated by UV radiation fields, photoionized nebulae glow by emitting strong emission lines. Ionized H and He emit by recombinations with free electrons, producing familiar lines such as $H\alpha$, $H\beta$, He I $\lambda 5876$ and He II $\lambda 4686$ in the optical. Strong emission lines from heavy element ions are almost invariably CELs. For example, excited by impacts with thermal electrons, doubly ionized O^{2+} emits [O III] $\lambda\lambda 4959, 5007$ nebular lines in the optical, [O III] 52- and 88- μm fine-structure lines in the far-IR and O III] $\lambda\lambda 1661, 1666$ intercombination lines in the UV. Recombinations of heavy element ions followed by cascades to ground levels also produce emission lines, such as the O II M 1 at 4649 \AA emitted by recombinations of O^{2+} . Due to the abundance effects, except for a few lines excited by di-electronic recombination, recombination lines of heavy element ions are generally quite faint and detectable only in the optical. Consequently these lines are often loosely referred to as ORLs.

Most emission lines of interest for plasma diagnostics and abundance determinations are optically thin, thus their observed intensities are proportional to emissivity defined as the energy emitted per ion per electron per unit time, $I(\lambda) \propto \epsilon(\lambda)N(X)N_e$, where $N(X)$ is the number density of the parent ionic species responsible for the emission of line λ . For example, both the [O III] $\lambda 5007$ CEL and O II $\lambda 4649$ ORL originate from doubly ionized oxygen, thus $N(X) = N(O^{2+})$ in both cases. By measuring intensity ratio of an ionic line relative to $H\beta$, $I(\lambda)/I(H\beta)$, the ionic abundance ratio, $N(X)/N(H^+)$, can be determined. Thus $N(O^{2+})/N(H^+)$ can be determined by measuring either the [O III] $\lambda 5007$ CEL or the O II $\lambda 4649$ ORL.

The behaviour of emissivity of a CEL as a function of T_e and N_e depends on two fundamental quantities – excitation energy E_{ex} and critical density N_c of the upper level of the transition (c.f. Osterbrock 1989): $\epsilon(\lambda) \propto T_e^{-1/2} \exp(-E_{\text{ex}}/kT_e)$, and $\epsilon(\lambda)$ is independent of N_e for $N_e \ll N_c$ and $\epsilon(\lambda) \propto N_e^{-1}$ for $N_e \gg N_c$. For [O III] $\lambda 5007$, $E_{\text{ex}} = 29,170$ K and $N_c = 6.9 \times 10^5 \text{ cm}^{-3}$, thus for a typical PN of $T_e \sim 10,000$ K and $N_e \leq 10,000 \text{ cm}^{-3}$, $\epsilon(\lambda 5007)$ is a strong function of T_e but essentially independent of N_e . By contrast, [O III] 52 μm has $E_{\text{ex}} = 440$ K and $N_c = 3,500 \text{ cm}^{-3}$, thus intensity of this line is almost independent of T_e but inversely proportional to N_e . Emissivities of all recombination lines have only a similar, weak power-law dependence on T_e and are essentially independent of N_e under typical nebular conditions. Emissivity of free to bound recombinations of ionized H and He with electrons, responsible for the weak nebular continuum observable in the optical and UV, also has a weak power-law dependence on T_e .

Figure 1 plots the emissivities of several ORLs and CELs as a function of T_e . Under typical nebular conditions, i.e. $T_e \sim 10,000$ K, collision excitation is several orders of magnitude more efficient in emitting a photon which cools the nebula. As T_e declines, the efficiency drops exponentially. Owing to their very low E_{ex} 's, far-IR FSLs such as [O III] 52 μm remain efficient coolants over a wide range of T_e , thus can cool the nebula down to a few hundred Kelvin. At such low temperatures, emission of recombination lines becomes significant, whereas optical CELs, such as [O III] $\lambda 5007$, disappear completely.

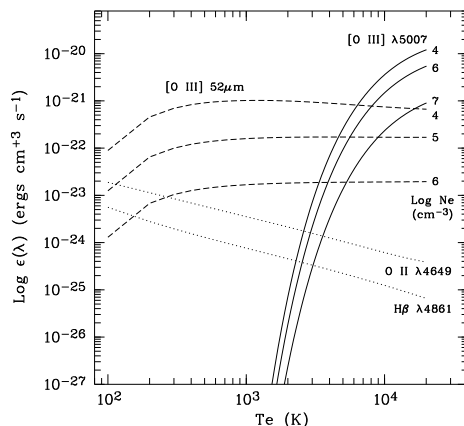


Fig. 1. Emissivities of H β and O II λ 4649 ORLs and [O III] λ 5007 and 52 μ m CELs as functions of T_e . Emissivities of ORLs are essentially independent of N_e . For CELs, curves for several values of N_e 's are shown.

3 Observations of ORLs

The high quality measurement and comprehensive analysis by Liu et al. (1995a) of the extraordinary rich and prominent O II permitted line spectrum of the Saturn nebula NGC 7009, which has been known for decades since the pioneer work of Wyse (1942), showed that $N(\text{O}^{2+})/N(\text{H}^+)$ derived from O II ORLs is a factor of 5 higher than derived from the [O III] $\lambda\lambda$ 4959,5007 CELs. Discrepancies of similar magnitude are also found for C and N and later for Ne (Luo et al. 2001). The problem is not new and has been known since the 1980s, as in the case of $N(\text{C}^{2+})/N(\text{H}^+)$ when comparing the values derived from the C II λ 4267 ORL and from the C III λ 1908 CEL. The study of Liu et al. (1995a) firmly established the ORL origin of those weak permitted lines and their legitimacy as abundance indicators, and ruled out measurement errors, blending by unknown lines and/or contamination of the relatively weak ORLs by excitation mechanisms other than recombination (e.g. fluorescence) as the cause of the discrepancies.

Since then, a deep spectroscopic survey for a large sample of Galactic PNe, aimed at determining nebular C/N/Oe abundances using ORLs and contrasting the results with values deduced from the traditional method based on CELs, has been carried out by the UCL group. Over a hundred PNe have been observed. For a 2 meter class telescope equipped with a long-slit spectrograph coupled with a high quantum efficiency CCD, ORLs from abundant second row elements can be measured in a few hours at a resolution of 3000 or better for bright Galactic PNe. The survey leads to the discovery of a rare group of PNe that exhibit extraordinary rich and prominent ORLs (Liu et al. 2000, 2001). Analyses of these PNe yield large discrepancies between the ORL and CEL abundances. In the most extreme case, the ORL abundances are nearly two orders of magnitude higher than the CEL values (c.f. Liu 2003 and references therein). Several dozen

PNe in the UCL sample have now been analyzed (Tsamis et al. 2003b, 2004; Liu et al. 2004ab; Wesson et al. 2004). Analysis for yet another subsample, comprising of over 30 Galactic bugle PNe, is currently in progress.

In the meanwhile, improved effective recombination coefficients have been calculated and published by the UCL group led by P. J. Storey for most abundant ions of second-row elements (O II, Storey 1994, Liu et al. (1995a); C II, Davey et al. 2000; N II, Kisielius & Storey 2002; Ne II, Kisielius et al. 1998, P. J. Storey, private communications). In these calculations, the effects of resonance recombinations are treated explicitly, therefore the published coefficients include contributions from both radiative and di-electronic recombinations. Radiative recombination and di-electronic recombination coefficients calculated with less sophisticated techniques for CNO ions are available from Péquignot et al. (1991) and Nussbaumer & Storey (1984), respectively.

Owing to the observational difficulty caused by low abundances as well as the lack of reliable atomic data, systematic abundance analyses using ORLs for third-row elements have yet to start. The only exception is magnesium. Due to its unusual large span in ionization potential, Mg^{2+} is often the most abundant ionic species of magnesium in a typical nebula. This combined with the fact that the recombined ion Mg II has only one active electron and thus a relatively simple spectrum, make the Mg II 3d–4f $\lambda 4481$ line relatively easy to detect. To a good approximation, one can assume that it has an effective recombination coefficient equal to that of the C II 3d–4f $\lambda 4267$ line. ORL abundances of magnesium have now been determined from the $\lambda 4481$ line for a number of PNe.

Dinerstein and Garnett (2001) surveyed two dozen PNe at a relatively low spectral resolution ($R \sim 2000$) and detected O II ORLs in ten of them. High quality echelle spectra aimed at ORL abundance analysis are published by the UNAM and IAC group for a number of bright Galactic H II regions and PNe (M 42, Esteban et al. 1998; M 17, Esteban et al. 1999a; M 8, Esteban et al. 1999b; NGC 5307, Ruiz et al. 2003; NGC 5315, Peimbert et al. 2004). Tsamis et al. (2003a) measured ORLs from CNO ions for three Galactic H II regions (M 42; M 17 and NGC 3576) and the giant H II regions 30 Doradus and N 11B in LMC and N 66 in SMC. Pushing to the limit of a four-metre class telescope, Esteban et al. (2002) measured O II ORLs from two giant H II regions in M 101 (NGC 5461 and 5471), one in M 33 (NGC 604) and another in NGC 2363. Detecting heavy element ORLs from H II regions is generally more difficult than from PNe, given the generally lower surface brightness of H II regions. The measurements are often complicated by comtaminations of scattered starlight from early type stars in the region. ORLs used for nebular abundance determinations are also present in spectra of early type stars, but in absorption rather than in emission.

4 Abundances Deduced from ORLs and CELs

Figure 2a plots the histogram of O^{2+}/H^+ logarithmic abundance discrepancy factor (adf), defined as the ratio of the ionic abundances derived from ORLs and from CELs, $\text{adf}(\text{O}^{2+}) \equiv [\text{O}^{2+}/\text{H}^+]_{\text{ORL}}/[\text{O}^{2+}/\text{H}^+]_{\text{CEL}}$, for 60 PNe. The sample

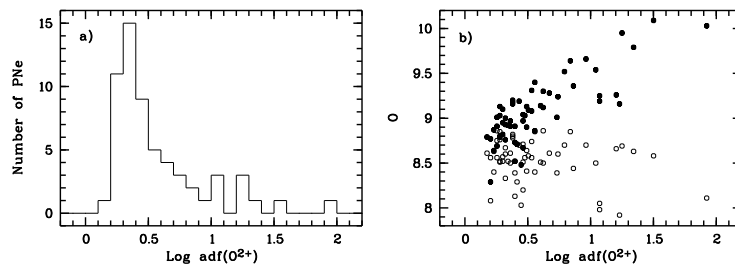


Fig. 2. a) Histogram of logarithmic abundance discrepancy factor (adf) for O^{2+}/H^+ ionic abundance ratio; b) Oxygen elemental abundance (in units where $H = 12$) derived from ORLs (filled circles) and from CELs (open circles) plotted against $\text{Log adf}(O^{2+})$.

includes 12 Galactic, 2 LMC and 1 SMC PNe analyzed by Tsamis et al. (2004), 10 Galactic PNe by Liu et al. (2004b), 22 by Wesson et al. (2004), M 2-24 and NGC 7027 by Zhang & Liu (2003) and Zhang, Liu & Luo (2004), NGC 6543 by Wesson & Liu (2004), Me 1-1 by Shen, Liu & Danziger (2004), NGC 5307 by Ruiz et al. (2003), NGC 5315 by Peimbert et al. (2004), NGC 1501 by Ercolano et al. (2004) and several Galactic PNe by Liu et al. (NGC 7009, M 1-42, M 2-36, NGC 6153, Hf 2-2; c.f. Liu 2003 and references therein).

Figure 2a shows that for all sampled PNe, $\text{Log adf}(O^{2+}) > 0$, i.e. O^{2+}/H^+ derived from ORLs is always higher than the value given by CELs. For the current sample, $\text{adf}(O^{2+})$ ranges from a factor of 1.5 to 84, peaking strongly at 0.35 dex (or factor of 2). About 10% of the sampled PNe have an $\text{adf}(O^{2+})$ in excess of 10.

Two out of the three Magellanic Cloud PNe (LMC N 141 and SMC N 87) have $\text{adf}(O^{2+}) = 2.6$ and 2.8, respectively, whereas the extraordinary LMC N 66, whose central star recently underwent a violent mass loss event, shows a large $\text{adf}(O^{2+})$ of 11. Although the sample is too small to make a general statement, it appears that Magellanic Cloud PNe also show a wide range of adf's. With the wide deployment of 10-m class telescopes, measuring adf's for a large sample of Magellanic Cloud PNe should become feasible.

$H\ II$ regions have also been found to have adf's always larger than unity, they seem to exhibit smaller adf's compared to PNe. For the limited number of Galactic and extragalactic $H\ II$ regions analyzed so far (c.f. references given in the previous section), the measured $\text{adf}(O^{2+})$'s fall in a relatively narrow range from 1.3 to 2.4 except for the low excitation LMC N 11B, which shows a large adf of 6 (Tsamis et al. 2003a) but with a large uncertainty.

In Fig. 2b, total oxygen elemental abundances derived from ORLs and from CELs are plotted against adf. Albeit with significant scatter, oxygen abundances deduced from CELs fall in a relatively narrow range, from 7.92 to 8.86, with an average value of 8.54 and a standard deviation of 0.23 in logarithmic scale where $H = 12$. Excluding the three Magellanic Cloud PNe, the halo PN DdDm 1 ($O = 8.05$; Wesson et al. 2004) and the peculiar PN M 2-24 ($O = 7.92$, the lowest amongst the sampled PNe; Zhang & Liu 2003), the mean CEL oxygen abun-

dance for the remaining 57 PNe is 8.57, slightly lower than the solar photospheric value of 8.69. This is consistent with the traditional understanding that PNe are descendants of low- and intermediate-mass Pop II stars and that oxygen abundance is largely unaffected by nucleosynthesis and various dredge-up processes that have occurred in progenitor stars.

In contrast, ORL oxygen abundances show a much wider range, reaching 10.09 in the most extreme case (NGC 1501). Amongst the 60 sampled PNe, four have oxygen ORL abundances in excess of ten times solar (M 1-42, NGC 40, Hf 2-2 and NGC 1501), yet except for Hf 2-2 which has a relatively low oxygen CEL abundance of 8.11, the oxygen CEL abundances of the other three PNe fall in a narrow range between 8.58 and 8.69. All the four PNe have an $\text{adf}(\text{O}^{2+})$ larger than 10. It is clear that the very high adf 's of these extreme PNe are entirely caused by their very high ORL abundances. Since ionic abundances derived from ORLs are essentially independent of the nebular thermal and density structures (Fig. 1), physically they should be more reliable than the CEL results, which depend strongly on T_e and N_e and are sensitive to possible existence of temperature and density inhomogeneities. On the other hand, the very high oxygen ORL abundances derived for some nebulae cast doubt on their legitimacy if the high abundances are indeed representative of the whole ejected PN envelopes.

It has been realized since the earlier study of NGC 7009 (Liu et al. 1995a; Luo et al. 2001) that adf 's larger than unity are observed in all abundant second-row elements, C, N, O and Ne, with comparable magnitudes for a given nebula. Interestingly, similar enhancement in ORL abundances has not been detected in magnesium, the only third-row element studied so far using an ORL (Barlow 2003). Of the 60 sample PNe, Mg abundances have been determined from the Mg II $\lambda 4481$ ORL for 26 of them. Excluding the peculiar bulge PN M 2-24 which has an abnormally high Mg abundance of 8.38, the Mg abundances of the remaining 25 PNe range from 7.27 to 7.88, with an average value of 7.51 and a standard deviation of 0.17. The average abundance is thus almost identical to the solar value of 7.54. Barlow et al. (2003) argue that depletion of magnesium onto dust grains is unlikely to be important for ionized regions of PNe. The stark contrast between Mg and second row elements should hold important clues to the nature and origin of the postulated ultra-cold ionized H-deficient clumps suspected to be embedded in PNe (c.f. next section for more details).

Garnett & Dinerstein (2001) find that larger, lower-surface brightness PNe tend to have adf 's greater than compact, dense ones. The result is supported by our high quality measurements for a large sample of PNe. It is found that adf is anticorrelated with $\text{H}\beta$ surface brightness, electron density and excitation class and positively correlated with nebular diameter. The scatter is large however in each case. Clearly while the problem of ORL to CEL abundance discrepancy is ubiquitous amongst PNe, it seems to become more profound or visible during the later evolutionary stages of PNe.

Only three PNe have been mapped in ORLs using long-slit spectroscopy. In all cases, adf is found to be strongly peaked at nebular centre, c.f. Liu (2003) for a recent review. No new data have been published since then. It is crucial to

extend observations to more PNe using higher angular resolutions. The recent deployment of 3D spectrographs on 10-m class telescopes should have a major impact on this area.

5 Temperature, Density and Abundance Inhomogeneities

Our extensive deep spectroscopic survey for a large sample of Galactic PNe has led to the discovery of a number of nebulae exhibiting unusual rich and prominent ORLs from ionized CNe ions. Detailed abundance analyses show that the heavy elemental abundances of these nebulae deduced from ORLs are often over an order of magnitude higher than those derived from CELs (c.f. Fig. 2a). All these nebulae have very low $T_e(\text{BJ})$'s, the Balmer jump temperatures derived from the nebular continuum Balmer discontinuity of hydrogen recombination spectrum, much lower than $T_e([\text{O III}])$'s, the temperatures derived from the $[\text{O II}]$ nebular to auroral line ratio (Liu et al. 2000, 2001b). The ORL to CEL abundance ratio is found to be tightly correlated with the difference between the two temperatures, $T_e([\text{O III}]) - T_e(\text{BJ})$ (Liu et al. 2001).

Detailed UV to far-IR multi-waveband abundance studies contrasting ionic abundances derived from ORLs and from CELs, first carried out by Liu et al. for NGC 6153 and then for two bulge PN M 1-42 and M 2-36, have now been carried out for a large number of PNe (Tsamis et al. 2004; Liu et al. 2004b; Wesson et al. 2004). The analyses confirm the earlier findings that FSLs, which have $E_{\text{ex}} \leq 1000$ K, generally yield ionic abundances in good agreement with values given by UV and/or optical CELs and therefore rule out temperature fluctuations of the type envisaged by Peimbert (1967) as the major cause of the ORL to CEL abundance discrepancy (Liu et al. 2000).

The $[\text{O III}]$ 52- and 88- μm lines have relatively low critical densities (3470 and 500 cm^{-3} , respectively), therefore their emission can be suppressed if the nebula has large density inhomogeneities and contains a substantial amount of ionized gas in dense clumps with N_e significantly higher than a few thousand cm^{-3} . Density inhomogeneities at modest levels are known amongst PNe (Liu et al. 2001a). On the other hand, a number of the sample PNe have N_e well below the critical density of the $[\text{O III}]$ 52- μm line, yet showing large values of adf. Examples of such PNe include M 1-42 [$N_e = 1200 \text{ cm}^{-3}$, $\text{adf}(\text{O}^{2+}) = 22$; Liu et al. 2001b], NGC 40 [$N_e = 1200 \text{ cm}^{-3}$, $\text{adf}(\text{O}^{2+}) = 18$; Liu et al. 2004b], NGC 2022 [$N_e = 1500 \text{ cm}^{-3}$, $\text{adf}(\text{O}^{2+}) = 16$; Tsamis et al. 2004], NGC 3132 [$N_e = 550 \text{ cm}^{-3}$, $\text{adf}(\text{O}^{2+}) = 2.4$; Tsamis et al. 2004], NGC 6720 [$N_e = 500 \text{ cm}^{-3}$, $\text{adf}(\text{O}^{2+}) = 2.4$; Liu et al. 2004b]. The large adf's observed in these low-density PNe are difficult to explain by the combined effects of density inhomogeneities and temperature fluctuations, as proposed by Ruiz et al. (2003) and Peimbert et al. (2004) for the high-density nebulae NGC 5307 and 5315. In addition, there are other FSLs of high N_e 's. For example, the $[\text{Ne III}]$ 15.5- μm line has a N_c of $2.0 \times 10^5 \text{ cm}^{-3}$, yet in almost all PNe studied, it yields a $\text{Ne}^{2+}/\text{H}^+$ abundance ratio consistent with that derived from the $[\text{Ne III}]$ $\lambda 3868$ CEL, rather than with the higher value derived from Ne II ORLs.

Zhang et al. (2004) determine T_e and N_e simultaneously for a large sample of PNe by fitting the H I recombination spectrum (including line and continuum emission such as the Balmer discontinuity and Balmer decrement) and compare the results with those derived from various optical/IR CEL diagnostic ratios. While the results yield strong evidence suggesting that both temperature fluctuations and density inhomogeneities at modest levels are generally present in PNe, it is clear that the differences between $T_e([\text{O III}])$ and $T_e(\text{BJ})$ observed in PNe of extreme adf values are so large that they cannot be explained in terms of temperature fluctuations of the type proposed by Peimbert (1967).

Several attempts to detect temperature fluctuations by mapping the spatial variations of $T_e([\text{O III}])$ via either direct monochromatic imaging or long-slit spectroscopy have been published. Using HST WFPC2 narrow-band images in the light of the $[\text{O III}] \lambda 5007$ and $\lambda 4363$ lines, after careful subtraction of contaminations by nebular continuum and nearby $\text{H}\gamma$, Rubin et al. (2002) and Wesson & Liu (2004) mapped the $\lambda 5007/\lambda 4363$ ratio and the resultant $T_e([\text{O III}])$ across the surface of NGC 7009 and NGC 6543, respectively. The resultant T_e varies in a narrow range, yielding a surface temperature fluctuations parameter t_A^2 of less than 0.01. For NGC 7009, the results are further corroborated by STIS long-slit spectroscopy. Note that although the measurements yield only mean electron temperatures integrated along the line of sight, under the reasonable assumption of random temperature fluctuations, as implied by the concept, one expects t_A^2 to be of similar magnitude of the true temperature fluctuation parameter t^2 . Thus for both nebulae, the observed t_A^2 values are too small to reconcile the large ORL to CEL abundance discrepancies, about a factor of 4.7 and 4.2 in NGC 7009 and 6543, respectively (Liu et al. 1995a; Wesson & Liu 2004).

For the Orion Nebula, O'Dell, Peimbert & Peimbert (2003) determine t_A^2 using HST WFPC2 images, and find that it varies between 0.005 and 0.016. From HST STIS long-slit spectra, Rubin et al. (2003) measure $T_e([\text{O III}])$ along several slit positions of the Orion Nebula and find a similar range of t_A^2 . Much earlier, from ground-based slit spectroscopy, Liu et al. (1995b) find that $T_e([\text{O III}]) \approx T_e(\text{BJ})$ and that both temperatures are nearly constant across the Orion Nebula, implying small temperature fluctuations. Note that the Orion Nebula has a small adf(O^{2+}) of only 1.3 (Esteban et al. 1998; Tsamis et al. 2003a), so it is not the best object to study the abundance discrepancy problem.

Liu et al. (2000) show that a two-abundance model incorporating a small amount of cold ionized H-deficient material can account for many of the observed patterns of NGC 6153 which has a large adf(O^{2+}) of 9.2. This is corroborated by the detailed photoionization models of Péquignot et al. (2002; 2003) and Tylenda (2003). In this scenario, the H-deficient gas is cooled to a few hundred Kelvin by recombinations and far-IR FSLs, compared to $\sim 10^4$ K in the main nebular component of “normal” chemical composition (i.e. about Solar). At such low temperatures, optical and UV CELs disappear almost entirely due to their very high E_{ex} 's, whereas emissivities of ORLs are enhanced. Only a small amount of H-deficient gas is required to account for the observed strengths of ORLs – in the particular model of NGC 6153 constructed by Péquignot et al., the H-deficient

Table 1. Comparison of ORL and CEL temperatures (K)

Nebula	$T_e([\text{O III}])$	$T_e(\text{H I BJ})$	$T_e(\text{He I ORLs})$	$T_e(\text{O II ORLs})$	adf(O^{2+})
Hf2-2	8820	900	775	630	84
M 1-42	9220	3560	2310	≤ 300	22
NGC 6153	9120	6080	3370	360	9.2
M 2-36	8380	5900	4160	520	6.9
NGC 7009	9980	8150	5380	420	4.7

component has a mass of only $0.0031 M_{\odot}$, about 1% of the total ionized mass of $0.38 M_{\odot}$ of the nebula. The H-deficient gas is enhanced in He and CNe heavy elements by a factor of 6 and 100, respectively. In this model, UV and optical CELs with high E_{ex} 's arise almost entirely from the hot nebular component, with a small contribution, at the level of a few per cent, *by recombinations*, from the cold H-deficient component. H I recombination lines are also dominated by emission from the normal component, with about 5% from the cold component leading to a lower value of $T_e(\text{BJ})$ compared to $T_e([\text{O III}])$. For He I ORLs, about 30% of the emission arises from the cold H-deficient component, whereas emission of heavy element ORLs arises almost entirely from the cold H-deficient component. An interesting aspect of this model is that because of tiny amount of gas in the H-deficient component, the average metallicity for the whole nebula is very close to that of the "normal" component as yielded by the traditional method of CEL abundance analysis. In the picture of two-abundance model, the small values of t_A^2 yielded by HST imaging or spectroscopy receive a natural explanation since as the H-deficient gas which has a very low T_e is "invisible" in the $[\text{O III}] \lambda 5007$ and $\lambda 4363$ lines.

The two-abundance (or H-deficient knot) model receives substantial support with the discovery of PNe exhibiting extremely low $T_e(\text{BJ})$'s, such as M 1-42 (3560 K; Liu et al. 2001) and Hf2-2 (900 K; Liu 2003). In both PNe, $T_e([\text{O III}]) \sim 9000$ K. This clearly shows that the nebula contains two phases of ionized gas, each with distinct physical conditions. Further evidence in support of the two-abundance model was presented by Liu (2003) who determined the *average* emission temperatures of He I and heavy element ORLs by comparing the observed intensity ratios with those predicted by recombination theory. Given that the weak dependence of intensity ratios of ORLs on T_e , measurements of very high accuracy are required. Analyses show that $T_e(\text{He I ORLs}) < T_e(\text{BJ})$, suggesting that He I lines have a lower average emission temperature than H I lines. Even lower T_e 's are yielded by O II and C II ORL ratios, reaching just a few hundred Kelvin in extreme cases such as Hf2-2 and M 1-42. Similar analyses have now been extended to a number of PNe (Tsamis et al. 2004; Liu et al. 2004b and Wesson et al. 2004), again yielding similar results. Table 1 presents example measurements of ORL and CEL temperatures for several PNe. Values

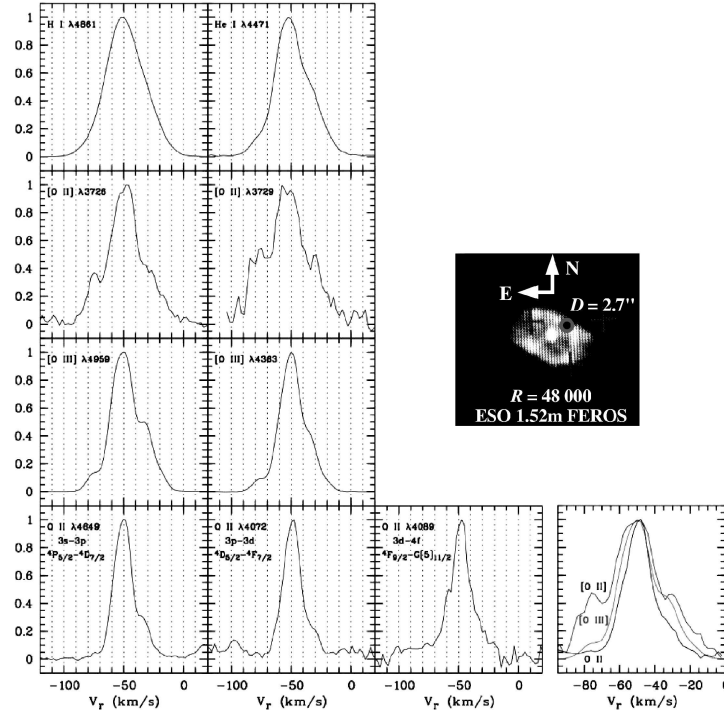


Fig. 3. CEL and ORL profiles in NGC 7009. The [O III] CELs and O II ORLs originate from the same O^{2+} ion, yet the O II ORLs are noticeably narrower.

of T_e (O II ORLs) have been rederived from the observed O II $\lambda 4089/\lambda 4649$ ratio using the most recent calculations of the effective recombination coefficients for O II, down to temperatures as low as 300 K, by P. J. Storey (c.f. Fig. 7 in Tsamis et al. 2004). The observed temperature sequence is in complete agreement with the expectation of the two-abundance model, which predicts that $T_e([O III]) > T_e(H I B J) > T_e(He I ORLs) > T_e(CN ONe ORLs)$ (Liu 2003; Péquignot et al. 2003). Note that the two-abundance model, which proposes a two phase nebula, each phase of ionized gas has a distinct chemical composition and temperature, is physically different to the picture of temperature fluctuations originally proposed by Peimbert (1967). As pointed out by Zhang, Liu & Liu (2004), in the scenario of temperature fluctuations, one expects $T_e(H I B J) < T_e(He I ORLs)$, exactly opposite to what observations yield.

Evidence in favour of a new component of ultra cold plasma emitting heavy element ORLs is also provided by high spectral resolution observations of weak ORLs, now starting to become available. In Fig. 3 we compare the observed line profiles of [O II] and [O III] CELs and H I, He I and O II ORLs, measured at a resolution of $R = 48,000$ with the FEROS spectrometer on the ESO 1.52m telescope. The very broad widths of H I and He I lines are apparently caused by

thermal broadening which is significant for light element ions. The [O II] CELs are broader than the [O III] CELs, in line with the expectation that the former arise from the outer, lower ionization regions. The most interesting feature revealed by Fig. 3 is that although both the [O III] and O II lines originate from the same O^{2+} ion, the O II ORLs are noticeably narrower, suggesting that the O II ORLs arise either from much cooler plasmas (thus have a smaller thermal broadening) or from spatially distinct regions than the [O III] lines. Ultra deep echelle spectrum of the low ionization PN IC418 at a resolution of 9 km s^{-1} has recently been obtained by Sharpee et al. (2004). They find that while O II lines are narrower than [O II] lines, they have widths comparable to those of [O III] lines. Given the very small adf's found for this high surface brightness PN [$\text{adf}(O^{2+}) = 1.3$], and the fact that the spectrum was an integration over a 6.5 arcsec slit length of 1 arcsec wide, it is probably of no surprise that [O III] CELs and O II ORLs have comparable line widths. In the likely case that the large adf's observed in other PNe are caused by the accumulated effects of a large number of small H-deficient knots, high spectral resolution *and* high spatial resolution spectroscopic observations are needed to detect possible differences in line width between [O III] CELs and O II ORLs.

6 Origins of the Ultra-Cold H-Deficient Plasmas

H-deficient knots are known to exist in a rare class of old PNe, including Abell 30, 58 and 78, IRAS 15154-5258 and 18333-2357 (e.g. Harrington 1996). In Abell 30, the H-deficient knots include two point-symmetric polar knots in $PA = 331^\circ$ at angular distances of 6.66 and 7.44 arcsec from the central star, plus a number of knots loosely outlining an inner equatorial ring. The knots are embedded in a round limb-brightened faint nebula of angular diameter of 127 arcsec. Deep spectroscopy of the two polar knots J 1 and J 3 by Wesson, Liu & Barlow (2003) reveals prominent ORLs from CNe ions almost identical to those observed in PNe such as NGC 7009 and 6153. Analyses yield $\text{adf}(O^{2+}) = 766$, $T_e([O \text{ III}]) = 17\,960 \text{ K}$, $T_e(\text{He I}) = 4600 \text{ K}$, $T_e([O \text{ II}]) = 450 \text{ K}$ for J 1 and $\text{adf}(O^{2+}) = 598$, $T_e([O \text{ III}]) = 16\,680 \text{ K}$, $T_e(\text{He I}) = 8840 \text{ K}$, $T_e([O \text{ II}]) = 2450 \text{ K}$ for J 3. In both knots oxygen has an abundance comparable to hydrogen by number, whereas helium abundance is about an order of magnitude higher. Thus the knots in Abell 30 exhibit many characteristics similar to those H-deficient knots hypothesized to exist in nebulae such as NGC 6153 and M 1-42, except that hydrogen in the knots of Abell 30 appears to be almost completely depleted.

A photoionization model for the H-deficient knot J 3 in Abell 30 has been constructed by Ercolano et al. (2003) using the newly developed 3D Monte Carlo photoionization code MOCASSIN. In spite of the much simplified nature of the model, such as neglecting the diffuse radiation field of the main nebula in which the knot is embedded, the model reproduces many features of the observations. In particular it shows that the metal-rich inner core of the knot has a T_e of only 500 K, in good agreement with the result of diagnostic analysis using O II ORLs. Interestingly, both the empirical analysis and the photoionization model

show that the knot is O-rich, rather than C-rich as suggested by earlier studies using CELs, in contradiction with the expectation of the “born-again” scenario proposed for the origin of PNe with H-deficient knots.

High resolution HST imaging has revealed that micro structures such as knots, filaments and clumps are ubiquitous in PNe (e.g. O’Dell et al. 2002). The nearby Helix nebula contains thousands of cometary globules, currently being ionized and evaporated by the strong radiation fields from the central star. Each of the knots contains a mass of gas of the order of the Earth (i.e. about $1 \times 10^{-6} M_{\odot}$), and has a dusty molecular core of H_2 and CO. The nature and origin of these knots remain a matter of debate. In particular the question of whether they are enhanced in heavy elements, and thus represent nearby examples of the H-deficient knots hypothesized to be posited in other PNe such as NGC 6153, M1-42 and Hf2-2 that cause the large adf values observed in those nebulae, remains to be investigated by deep spectroscopic observations. At the moment, direct observational evidence pointing towards the existence of such H-deficient knots in these extreme PNe is still lacking. Torres-Peimbert, Peimbert & Peña (1990) suggested that the large $adf(C^{2+})$ observed in the halo PN NGC 4361 could be caused by a C-rich inner shell where the C/H abundance is 100 times than the outer region, resulting a lower T_e of 11,400 K in the inner shell compared to 20,200 K in the outer region. Using deep long-slit spectroscopy, Liu (1998) mapped carbon ORLs across the nebula at a spatial resolution of $4.9 \times 2 \text{ arcsec}^2$ and failed to detect a C-rich inner zone. While the observation ruled out the two-zone model proposed by Torres-Peimbert et al., it did not rule out the possibilities of small metal-rich clumps well embedded in the nebula.

While there seems good evidence suggesting that there is another component of ultra-cold ionized H-deficient gas in PNe, probably in the form of numerous H-deficient knots, the nature and origin of such knots remain a mystery. It is not clear whether they are nucleo-processed material, as proposed for the H-deficient knots in Abell 30. It seems that the knots are enhanced in He and CNO, but not in Mg. An alternative to the scenario of nucleo-processed material ejected by the progenitor star is that the knots are planets, planetesimals and comets of the planetary system of the progenitor star being ionized, stripped off and evaporated by the radiation field and stellar wind from the host star that is now evolving to become a white dwarf (Liu 2003). Analyses of PNe such as NGC 6153 and M1-42 show that only a few Jupiter masses of metal-rich material is required to explain the strengths of ORLs observed in these nebulae, so the idea may not be so eccentric as it first looks. Evaporating proto-planetary disks around newly formed stars in H II regions (such as the proplyds in M42) may likewise provide a natural solution to a similar ORL/CEL abundance discrepancy problem observed to be widely present in H II regions (Liu 2003).

The possible existence of H-deficient knots in ionized nebulae could potentially have a profound consequence on He abundances of PNe and H II regions, and on the primordial He abundance determined by extrapolating He abundances of metal-poor H II galaxies to zero metallicity (Zhang et al. 2004). Péquignot et al. (2002; 2003) and Liu (2003) noticed that in the two-abundance

scenario, He abundance is least constrained by observations, since all strong He lines measurable in the optical and UV are dominated by recombination excitation, and thus can be strongly contaminated by emission from the small amount of H-deficient ultra-cold plasma posited in the nebula. For NGC 6153, two-abundance photoionization modelling by Péquignot et al. (2002; 2003) shows that, after averaging over the entire volume of ionized gas, the nebula has a helium abundance of 0.101, essentially identical to the Solar value but much lower than the value of 0.136 derived from empirical analysis assuming a chemically homogeneous nebula (Liu et al. 2000). The lower helium abundance in NGC 6153 is supported by our measurement of the He I $\lambda 10830$ line, for which collision by electron impacts from the $2s^3S$ meta-stable level has a major contribution to its observed flux.

References

1. M. J. Barlow, X.-W. Liu, D. Péquignot, P. J. Storey, Y. G. Tsamis, C. Morisset: In: *Planetary Nebulae: Their Evolution and Role in the Universe, IAU Symp. 209, Canberra, Australia, 19-23 Nov. 2001*, ed. by S. Kwok, M. Dopita, R. Sutherland (Pub. Astr. Soc. Pacific, 2003), p.373
2. A. R. Davey, P. J. Storey, R. Kisielius: *A&AS*, **142**, 85 (2000)
3. B. Ercolano, M. J. Barlow, P. J. Storey, et al.: *MNRAS*, **344**, 1145 (2003)
4. B. Ercolano, R. Wesson, Y. Zhang, et al.: *MNRAS*, in press (astro-ph/0407230; 2004)
5. C. Esteban: *RMxAA (Conf. Ser.)*, **12**, 56 (2002)
6. C. Esteban, M. Peimbert, S. Torres-Peimbert, V. Escalante: *MNRAS*, **295**, 401 (1998)
7. C. Esteban, M. Peimbert, S. Torres-Peimbert, J. García-Rojas: *RMxAA*, **35**, 65 (1999a)
8. C. Esteban, M. Peimbert, S. Torres-Peimbert, et al.: *ApJS*, **120**, 113 (1999b)
9. C. Esteban, M. Peimbert, S. Torres-Peimbert, M. Rodríguez: *ApJ*, **581**, 241 (2002)
10. G. Ferland: *ARAA*, **41**, 517 (2003)
11. D. R. Garnett, H. L. Dinerstein: *RMxAA (Conf. Ser.)*, **10**, 13 (2001)
12. J. P. Harrington: In: *Hydrogen-Deficient Stars, ASP Conf. Ser. Vol. 96*, ed. by C. S. Jeffery, U. Hebera (Pub. Astron. Soc. Pac., San Francisco, 1996), p.193
13. R. Kisielius, P. J. Storey: *A&A*, **387**, 1135 (2002)
14. R. Kisielius, P. J. Storey, A. R. Davey, L. T. Neale: *A&AS*, **133**, 257 (1998)
15. X.-W. Liu: *MNRAS*, **295**, 699 (1998)
16. X.-W. Liu: *RMxAA (Conf. Ser.)*, **12**, 70 (2002)
17. X.-W. Liu: In: *Planetary Nebulae: Their Evolution and Role in the Universe, IAU Symp. 209*, ed. by S. Kwok, M. Dopita, R. Sutherland (Pub. Astr. Soc. Pacific, 2003), p.339
18. X.-W. Liu, M. J. Barlow, M. Cohen, I. J. Danziger, S.-G. Luo, J. P. Baluteau, et al.: *MNRAS*, **323**, 343-361 (2001a)
19. X.-W. Liu, M. J. Barlow, I. J. Danziger, P. J. Storey: *ApJ*, **450**, L59 (1995b)
20. X.-W. Liu, S.-G. Luo, M. J. Barlow, et al.: *MNRAS*, **327**, 141 (2001b)
21. X.-W. Liu, P. J. Storey, M. J. Barlow, R. E. S. Clegg: *MNRAS*, **272**, 369 (1995a)
22. X.-W. Liu, P. J. Storey, M. J. Barlow, et al.: *MNRAS*, **312**, 585 (2000)
23. Y. Liu, X.-W. Liu, S.-G. Luo, Barlow M. J.: *MNRAS*, in press (2004a)

24. Y. Liu, X.-W. Liu, M. J. Barlow, S.-G. Luo: MNRAS, in press (2004b)
25. S.-G. Luo, X.-W. Liu, M. J. Barlow: MNRAS, **326**, 1049 (2001)
26. H. Nussbaumer, P. J. Storey: A&AS, **56**, 293 (1984)
27. C. R. O'Dell, B. Balick, A. R. Hajian, et al.: AJ, **123**, 3329 (2002)
28. C. R. O'Dell, M. Peimbert, A. Peimbert: AJ, **125**, 2590 (2003)
29. D. Osterbrock: *Astrophysics of Gaseous Nebulae and Active Galactic Nuclei* (University Science Books, Mill Valley, 1989)
30. M. Peimbert: ApJ, **150**, 825 (1967)
31. M. Peimbert: RMxAA (Conf. Ser.), **12**, 275 (2002)
32. M. Peimbert, A. Peimbert, M. T. Ruiz, C. Esteban: ApJS, **150**, 431 (2004)
33. D. Péquignot, M. Amara, X.-W. Liu, et al.: RMxAA (Conf. Ser.), **12**, 142 (2002)
34. D. Péquignot, X.-W. Liu, M. J. Barlow, et al.: In: *Planetary Nebulae: Their Evolution and Role in the Universe, IAU Symp. 209*, ed. by S. Kwok, M. Dopita, R. Sutherland (Pub. Astr. Soc. Pacific, 2003), p.347
35. D. Péquignot, P. Petitjean, C. Boisson: A&A, **251**, 680 (1991)
36. R. Rubin, N. J. Bhatt, R. J. Dufour, et al.: MNRAS, **334**, 777 (2002)
37. R. Rubin, P. G. Martin, R. J. Dufour, et al.: MNRAS, **340**, 362 (2003)
38. M. T. Ruiz, A. Peimbert, M. Peimbert, C. Esteban: ApJ, **595**, 247 (2003)
39. B. Sharpee, J. A. Baldwin, R. Williams: ApJ, in press (astro-ph/0407186; 2004)
40. Z.-X. Shen, X.-W. Liu, I. J. Danziger: A&A, in press (2004)
41. P. J. Storey: A&A, **282**, 999
42. S. Torres-Peimbert, M. Peimbert, M. Peña: A&A, **233**, 540
43. Y. G. Tsamis, M. J. Barlow, X.-W. Liu, et al.: MNRAS, **338**, 186 (2003a)
44. Y. G. Tsamis, M. J. Barlow, X.-W. Liu, I. J. Danziger, P. J. Storey: MNRAS, **353**, 953 (2004)
45. S. Torres-Peimbert, M. Peimbert:, In: *Planetary Nebulae: Their Evolution and Role in the Universe, IAU Symp. 209*, ed. by S. Kwok, M. Dopita, R. Sutherland (Pub. Astr. Soc. Pacific, 2003), p.363
46. R. Tylenda: In: *Planetary Nebulae: Their Evolution and Role in the Universe, IAU Symp. 209*, ed. by S. Kwok, M. Dopita, R. Sutherland (Pub. Astr. Soc. Pacific, 2003), p.159
47. R. Wesson, X.-W. Liu: MNRAS, **351**, 1026 (2004)
48. R. Wesson, X.-W. Liu, M. J. Barlow: MNRAS, **340**, 253 (2003)
49. R. Wesson, X.-W. Liu, M. J. Barlow: MNRAS, submitted (2004)
50. A. B. Wyse: ApJ, **95**, 356 (1942)
51. Y. Zhang, X.-W. Liu: A&A, **404**, 545 (2003)
52. Y. Zhang, X.-W. Liu, Y. Liu: in preparation (2004)
53. Y. Zhang, X.-W. Liu, S.-G. Luo: in preparation (2004)
54. Y. Zhang, X.-W. Liu, R. Wesson, et al.: MNRAS, **351**, 935 (2004)